An Accelerated Coupled Feed-Radiator-Frequency Selective Surface Model for the Next Generation Active Phased Array Systems

B.J. Morsink[(1)], G.H.C. van Werkhoven[(2)], A.G. Tijhuis[(3)] and S.W. Rienstra[(4)]

[(1)]Thales Naval Nederland, Business Unit Radar and Sensors, P.O. Box 42, 7550 GD, Hengelo (Ov.), The Netherlands, bart.morsink@nl.thalesgroup.com

[(2)]Thales Naval Nederland, Business Unit Radar and Sensors, P.O. Box 42, 7550 GD, Hengelo (Ov.), The Netherlands, gertjan.vanwerkhoven@nl.thalesgroup.com

[(3)]Faculty of Electrical Engineering, Eindhoven University of Technology, P.O. Box 513, 5600 MB Eindhoven, The Netherlands, a.g.tijhuis@tue.nl

[(4)]Faculty of Mathematics & Comp. Sc., Eindhoven University of Technology, P.O. Box 513, 5600 MB Eindhoven, The Netherlands, s.w.rienstra@tue.nl

INTRODUCTION

Thales Naval Nederland (TNN) has a great history in developing phased array radar systems for naval applications. The most recent innovative examples are the SMART-L long range 3D volume search radar and the APAR multi-function search/track and missile guidance radar. Recent activities include developments of active phased array antennas consisting of multilayer structures designed for a large scanning range, with a relatively large bandwidth and with low radar cross-section (RCS).

Within this context and in collaboration with the Eindhoven University of Technology, we have studied these design properties by analysing the electromagnetic behaviour of so-called combined feed-radiator-frequency selective surface type array antennas. More specific, but expressed in more general terms, a numerical model has been developed for the analysis of a stratified periodic electromagnetic field problem. In a previous paper [4], this model has been compared and benchmarked against available commercial tooling such as HFSS. An arbitrary structure has been analysed for its reflection and transmission properties. The emphasis in this paper however is on a new type of acceleration technique that is presented and implemented to reduce the computation time while maintaining accuracy.

FORMULATION OF THE PROBLEM

It is conventional to let the $\hat{z}$-axis point in the longitudinal direction. Accordingly, a so-called transverse plane is a plane for which z is arbitrary but fixed. In a given transverse plane the position is fully specified by the transverse part $\underline{\rho}$ of the position vector $\underline{r}$, which is given by $\underline{\rho} = \rho_x\hat{x} + \rho_y\hat{y}$ and $\underline{r} = \underline{\rho} + z\hat{z}$. The configuration is characterised separately in the transverse and longitudinal direction. In the transverse direction, we allow for a periodic arrangement in a skew lattice defined by the transverse basis vectors $\underline{d}_1$ and $\underline{d}_2$ of so-called unit-cells. In the longitudinal direction, within a unit-cell but equal over all unit-cells, we allow for an arbitrary stratification. Within this stratification, we can either place a frequency selective surface (FSS) or a waveguide (WG), both containing an arbitrary number of homogeneous dielectric layers and/or shaped metal sheets.

The electromagnetic field and current densities are written as functions of a combination of transverse components $\underline{\rho}$ and longitudinal components z in the point of observation $\underline{r}$. The electromagnetic field and current densities can be written in terms of transverse $\{\underline{E}_t, \underline{H}_t, \underline{J}_t, \underline{M}_t\}$ and longitudinal $\{E_z, H_z, J_z, M_z\}$ components. The electromagnetic field and current densities, located at an infinitesimal close distance towards the left side of any interface $z = z_m$, are denoted by $\{\hat{\underline{E}}_m, \hat{\underline{H}}_m, \hat{\underline{J}}_m, \hat{\underline{M}}_m\}$. Those located at the right side are denoted by $\{\check{\underline{E}}_m, \check{\underline{H}}_m, \check{\underline{J}}_m, \check{\underline{M}}_m\}$.

A single unit-cell of the configuration of interest is given in figure 1. It consists of three parts : a slot, box and an FSS. The slot is a waveguide with dimensions width w_s and height h_s. It is filled with a material with $\varepsilon_r = 3$ and $\mu_r = 1$. The box is a waveguide with dimensions width w_b, height h_b and depth d. It is filled with a material with $\varepsilon_r = 3$ and $\mu_r = 1$. The FSS is a periodic layered space. It consists of a slab with thickness s and is filled with a material with $\varepsilon_r = 1.24$ and $\mu_r = 1$. Between the box and the slab an infinitely thin perfectly electric conducting patch with dimensions width w_p and height h_p is placed. On top of the slab there is free space. The unit-cells are

0-7803-7827-X/03/$17.00 ©2003 IEEE.

placed in a rectangular grid with basis vectors $\underline{d}_1$ and $\underline{d}_2$. From a transverse point of view, all parts of this structure are centered within the unit-cell.

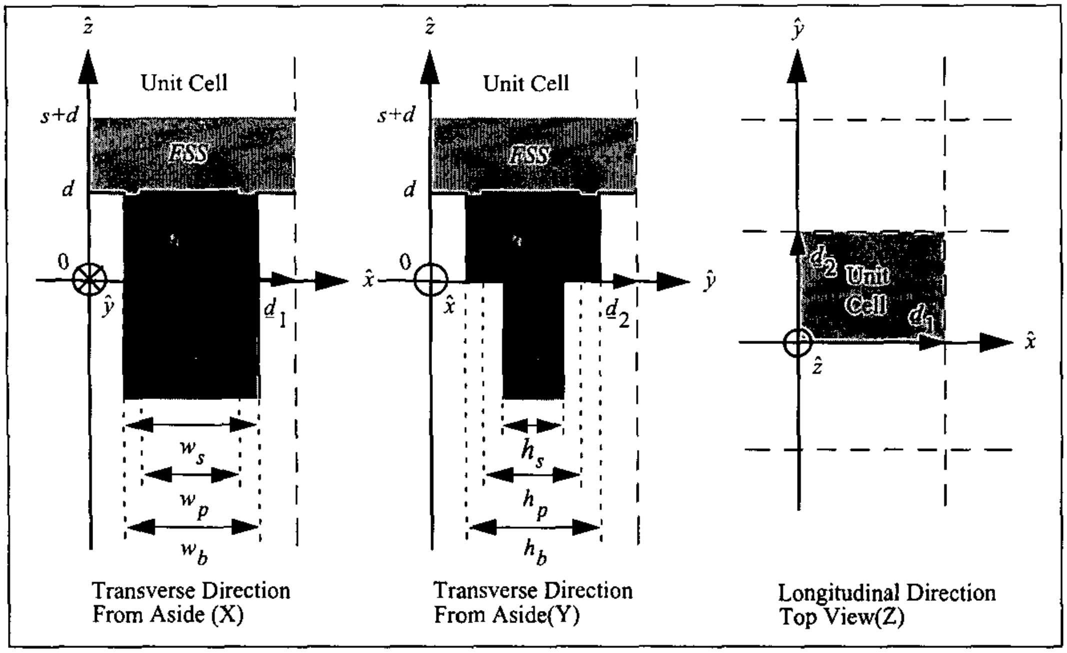

Figure 1. Description of the configuration of interest

The field problem is solved by solving a coupled magnetic field integral equation (MFIE) for all discontinuities at once. We exploit the analytical knowledge of the spectral Green's function both for the waveguide as well as for the periodic layered space, which in fact are two examples of stratified electromagnetic field problems.

BOUNDARY CONDITIONS

To ensure existence and uniqueness of the electromagnetic field quantities, the Maxwell's equations must be supplemented with boundary conditions that interrelate the field values at both sides of surfaces of discontinuity. The surfaces $\bar{S}_a$ and $\bar{S}_b$ indicated in figure 2 are such type of surfaces and are composed of infinitely thin perfectly electric conducting material. Consequently, the boundary conditions across these interfaces are given by

$$\forall \underline{\rho} \in \bar{S}_a[\tilde{\underline{E}}_{t;a} = \underline{0}] \qquad \forall \underline{\rho} \in \bar{S}_b[\tilde{\underline{E}}_{t;b} = \underline{0}] \tag{1}$$

The surfaces S_a and S_b represent the common openings. Consequently, the boundary conditions across these interfaces are given by

$$\forall \underline{\rho} \in S_a[\hat{\underline{E}}_{t;a} = \tilde{\underline{E}}_{t;a} \wedge \hat{\underline{H}}_{t;a} = \tilde{\underline{H}}_{t;a}] \qquad \forall \underline{\rho} \in S_b[\hat{\underline{E}}_{t;b} = \tilde{\underline{E}}_{t;b} \wedge \hat{\underline{H}}_{t;b} = \tilde{\underline{H}}_{t;b}] \tag{2}$$

FORMULATION OF AN EQUIVALENT FIELD PROBLEM

We introduce magnetic surface currents $\hat{\underline{M}}_a$ and $\tilde{\underline{M}}_a$ on interface S_a and $\hat{\underline{M}}_b$ and $\tilde{\underline{M}}_b$ on interface S_b. Interfaces S_a and S_b will be closed with infinitely thin perfectly electric conducting material. The equivalent problem has a unique solution if the following boundary conditions are satisfied. Across the surfaces $\bar{S}_a$ and $\bar{S}_b$ (see figure 2) boundary conditions 1 are translated into

$$\forall \underline{\rho} \in \bar{S}_a[\tilde{\underline{M}}_a = \underline{0}] \qquad \forall \underline{\rho} \in \bar{S}_b[\tilde{\underline{M}}_b = \underline{0}] \tag{3}$$

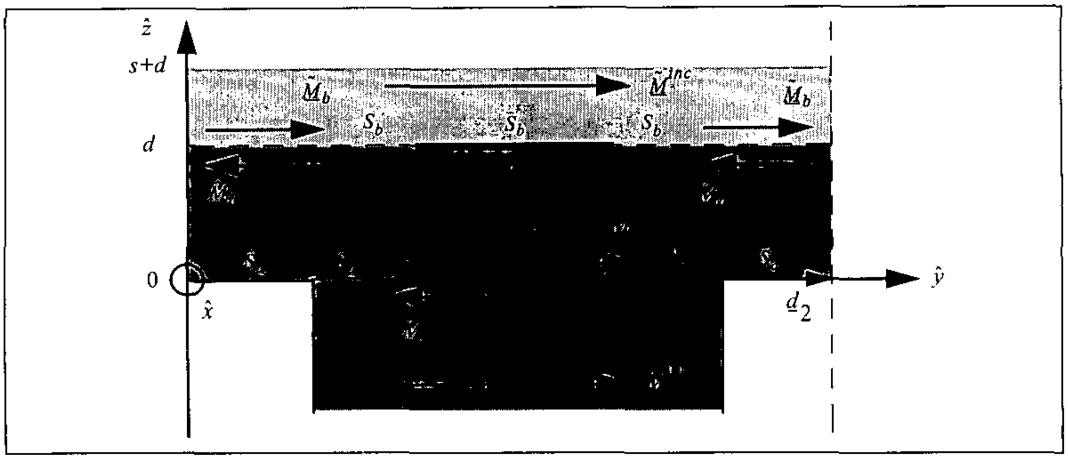

Figure 2. Boundary Conditions and the Equivalent Field Problem

Across the surfaces S_a and S_b boundary conditions 2 are translated into

$$\forall \underline{\rho} \in S_a[\tilde{\underline{M}}_a = -\hat{\underline{M}}_a \wedge \hat{\underline{H}}_{t;a} = \tilde{\underline{H}}_{t;a}] \qquad \forall \underline{\rho} \in S_b[\tilde{\underline{M}}_b = -\hat{\underline{M}}_b \wedge \hat{\underline{H}}_{t;b} = \tilde{\underline{H}}_{t;b}] \tag{4}$$

COUPLED MAGNETIC FIELD INTEGRAL EQUATION

At both interfaces S_a and S_b, boundary condition 4 can be written in terms of the unknown equivalent surface currents $\hat{\underline{M}}_a$, $\tilde{\underline{M}}_a$, $\hat{\underline{M}}_b$ and $\tilde{\underline{M}}_b$. When applying the superposition principle and boundary condition 3, we obtain the following coupled system of magnetic field integral equations with unknown surface currents $\hat{\underline{M}}_a$ and $\hat{\underline{M}}_b$

$$\forall \underline{\rho} \in S_a[\hat{\underline{H}}_{t;a}(\underline{0}, \hat{\underline{M}}_a) + \tilde{\underline{H}}_{t;a}(\hat{\underline{M}}_a, \underline{0}) - \tilde{\underline{H}}_{t;a}(\underline{0}, \hat{\underline{M}}_b) = -\hat{\underline{H}}_{t;a}(\hat{\underline{M}}^{inc}, \underline{0})] \tag{5}$$

$$\forall \underline{\rho} \in S_b[-\hat{\underline{H}}_{t;b}(\hat{\underline{M}}_a, \underline{0}) + \hat{\underline{H}}_{t;b}(\underline{0}, \hat{\underline{M}}_b) + \tilde{\underline{H}}_{t;b}(\hat{\underline{M}}_b, \underline{0}) = \tilde{\underline{H}}_{t;b}(\underline{0}, \tilde{\underline{M}}^{inc})] \tag{6}$$

METHOD OF MOMENTS

To solve the MFIE we used the method of moments (MoM). The unknown magnetic surface currents $\hat{\underline{M}}_a$ and $\hat{\underline{M}}_b$ are expanded and weighted in terms of Rao-Wilton-Glisson (RWG) basis functions. The unknown currents can be expanded as

$$\hat{\underline{M}}_a(\underline{\rho}) = \sum_m V_m^a g_m^a(\underline{\rho}) \qquad \hat{\underline{M}}_b(\underline{\rho}) = \sum_n V_n^b g_n^b(\underline{\rho}) \tag{7}$$

The weighting can be written in terms of a complex inner product $\langle \underline{f}(\underline{\rho}) | g(\underline{\rho}) \rangle$ (linear in its first term) as

$$\forall \underline{\rho} \in S_a[\underline{f}(\underline{\rho}) = \underline{0}] \Rightarrow \forall k[\langle \underline{f}(\underline{\rho}) | g_k^a(\underline{\rho}) \rangle = 0] \qquad \forall \underline{\rho} \in S_b[\underline{f}(\underline{\rho}) = \underline{0}] \Rightarrow \forall l[\langle \underline{f}(\underline{\rho}) | g_l^b(\underline{\rho}) \rangle = 0] \tag{8}$$

The following set of linear equations are obtained for the coupled magnetic field integral equations 5 and 6

$$\forall k\left[\sum_m V_m^a \langle \hat{\underline{H}}_{t;a}(\underline{0}, g_m^a) + \tilde{\underline{H}}_{t;a}(g_m^a, \underline{0}) | g_k^a \rangle - \sum_n V_n^b \langle \tilde{\underline{H}}_{t;a}(\underline{0}, g_n^b) | g_k^a \rangle = -\langle \hat{\underline{H}}_{t;a}(\hat{\underline{M}}^{inc}, \underline{0}) | g_k^a \rangle\right] \tag{9}$$

$$\forall l\left[-\sum_m V_m^a \langle \hat{\underline{H}}_{t;b}(g_m^a, \underline{0}) | g_l^b \rangle + \sum_n V_n^b \langle \hat{\underline{H}}_{t;b}(\underline{0}, g_n^b) + \tilde{\underline{H}}_{t;b}(g_n^b, \underline{0}) | g_l^b \rangle = \langle \tilde{\underline{H}}_{t;b}(\underline{0}, \tilde{\underline{M}}^{inc}) | g_l^b \rangle\right] \tag{10}$$

which can be rewritten in the following (admittance) matrix form

$$Y\underline{V} = \underline{I} \qquad Y = \begin{bmatrix} A_{k,m} + B_{k,m} & C_{k,n} \\ D_{l,m} & E_{l,n} + F_{l,n} \end{bmatrix} \qquad \underline{V} = \begin{bmatrix} V_m^a \\ V_n^b \end{bmatrix} \qquad \underline{I} = \begin{bmatrix} G_k \\ H_l \end{bmatrix} \tag{11}$$

SPECTRAL GREEN'S FUNCTION

In a waveguide the transverse electromagnetic field can be written as

$$\underline{E}_t(\rho, z) = \sum_{\alpha, m} V_m^{\alpha}(z)\underline{e}_m^{\alpha}(\underline{\rho}) \qquad \underline{H}_t(\rho, z) = \sum_{\alpha, m} I_m^{\alpha}(z)\underline{h}_m^{\alpha}(\underline{\rho}) \tag{12}$$

where α represents the polarization index, TM α = ' and TE polarization α = '', and m represents the waveguide mode index. In layered space the transverse electromagnetic field can be written as

$$\underline{E}_t(\rho, z) = \sum_{\alpha}\int \mathrm{d}\underline{k}_t \cdot V^{\alpha}(\underline{k}_t, z)\underline{e}^{\alpha}(\underline{k}_t, \underline{\rho}) \qquad \underline{H}_t(\rho, z) = \sum_{\alpha}\int \mathrm{d}\underline{k}_t \cdot I^{\alpha}(\underline{k}_t, z)\underline{h}^{\alpha}(\underline{k}_t, \underline{\rho}) \tag{13}$$

where α represents the polarization index and $\underline{k}_t$ represents the transverse wavevector. Note that the index m in the waveguide formulation and the vector $\underline{k}_t$ in the layered space formulation have a similar meaning. For the layered space, the transverse wavevectors can be written down in closed form.

$$\underline{e}'(\underline{k}_t, \underline{\rho}) = \frac{\mathrm{j}}{2\pi}\hat{k}_t e^{-\mathrm{j}\underline{k}_t \bullet \underline{\rho}} \qquad \underline{h}'(\underline{k}_t, \underline{\rho}) = -\frac{\mathrm{j}}{2\pi}\hat{\alpha}_t e^{-\mathrm{j}\underline{k}_t \bullet \underline{\rho}} \qquad \hat{k}_t = \underline{k}_t/\|\underline{k}_t\| \tag{14}$$

$$\underline{e}''(\underline{k}_t, \underline{\rho}) = \frac{\mathrm{j}}{2\pi}\hat{\alpha}_t e^{-\mathrm{j}\underline{k}_t \bullet \underline{\rho}} \qquad \underline{h}''(\underline{k}_t, \underline{\rho}) = \frac{\mathrm{j}}{2\pi}\hat{k}_t e^{-\mathrm{j}\underline{k}_t \bullet \underline{\rho}} \qquad \hat{\alpha}_t = \hat{k}_t \times \hat{z} \tag{15}$$

when combining 13 with 14 and 15, the spectral representation of the transverse electromagnetic field is recognised. The longitudinal components $V^{\alpha}(z)$ and $I^{\alpha}(z)$ satisfy the so-called transmission line equations.

USING PERIODICITY

The interface S_b is closed with metal, making the outer side at $z = d$ (see figure 2) the only place for the the unit cells to interact with eachother in this equivalent formulation. So this is the place to take into account the periodic character of the structure. We do this by making the unknown current $\tilde{\underline{M}}_b$ periodic in behaviour, i.e. we replace $\tilde{\underline{M}}_b$ with $\tilde{\underline{M}}_b^{per}$ in the magnetic field density $\tilde{\underline{H}}_{t;b}(\tilde{\underline{M}}_b, \underline{0})$. Since $\tilde{\underline{M}}_b = -\underline{M}_b$, the periodic expansion function for the outer side of this interface can now be written as

$$\tilde{\underline{M}}_b^{per}(\underline{\rho}) = -\sum_n V_n^b \underline{g}_n^{b;per}(\underline{\rho}) \tag{16}$$

The periodic expansion function $\underline{g}_n^{b;per}$ is formulated as a function of the non-periodic expansion function $\underline{g}_n^b$ as

$$\underline{g}_n^{b;per}(\underline{\rho}) = e^{-\mathrm{j}\underline{k}_t^i \bullet \underline{\rho}}\left[\left(\underline{g}_n^b(\underline{\rho})e^{\mathrm{j}\underline{k}_t^i \bullet \underline{\rho}}\right) * \Pi_{\underline{d}_1, \underline{d}_2}(\underline{\rho})\right] \qquad \Pi_{\underline{d}_1, \underline{d}_2}(\underline{\rho}) = \sum_{m_1, m_2 = -\infty}^{\infty} \delta(\underline{\rho} - m_1\underline{d}_1 - m_2\underline{d}_2) \tag{17}$$

where * denotes convolution with respect to $\underline{\rho}$. $\Pi_{\underline{d}_1, \underline{d}_2}$ denotes the so-called Dirac brush function. The spectral representation of the $\underline{g}_n^{b;per}$ can be expressed as (where $\underline{k}_1$ and $\underline{k}_2$ denote the reciprocal basis vectors)

$$\langle \underline{g}_n^{b;per} | \underline{h}^{\alpha}\rangle(\underline{k}_t) = \frac{4\pi^2}{A}\Pi_{\underline{k}_1, \underline{k}_2}(\underline{k}_t - \underline{k}_t^i)\langle \underline{g}_n^b | \underline{h}^{\alpha}\rangle(\underline{k}_t) \qquad \underline{k}_i \bullet \underline{d}_j = 2\pi\delta_{i,j} \tag{18}$$

ACCELERATION TECHNIQUE

Any contribution $A_{k,m}$ to the admittance matrix Y (see equation 11) can be written in the following general form as

$$A_{k,m} = \sum_{j,\alpha} h^{\alpha}(\underline{k}_{t;j})\hat{\beta}_{k,m}^{\alpha}(\underline{k}_{t;j}) \qquad \underline{k}_{t;j} = B\underline{m}_j + \underline{k}_t^i \qquad A^T B = 2\pi I \tag{19}$$

in which the matrices A and B respectively represent the direct and reciprocal lattice. For example

$$A_{k,m} = \langle \tilde{\underline{H}}_{t;a}(\underline{0}, \underline{g}_m^a) | \underline{g}_k^a\rangle = \sum_{j,\alpha} I^{\alpha}(\underline{k}_{t;j}, 0^-)\langle \underline{h}^{\alpha}(\underline{k}_{t;j}) | \underline{g}_k^a\rangle \qquad I^{\alpha}(\underline{k}_t, 0^-) = -Y_{\infty}^{\alpha}(\underline{k}_t)\langle \underline{g}_m^a | \underline{h}^{\alpha}(\underline{k}_t)\rangle \tag{20}$$

then the general form can be recognised if we take for $h^{\alpha}(\underline{k}_t)$ and $\hat{\beta}_{k,m}^{\alpha}(\underline{k}_t)$ the following

$$h^{\alpha}(\underline{k}_t) = -Y_{\infty}^{\alpha}(\underline{k}_t) \qquad \hat{\beta}_{k,m}^{\alpha}(\underline{k}_t) = \langle \underline{g}_m^a | \underline{h}^{\alpha}\rangle\langle \underline{h}^{\alpha} | \underline{g}_k^a\rangle \tag{21}$$

If we define

$$g^{\alpha}(k_t) = \begin{cases} h^{\alpha}(k_t) & \text{if } \alpha = TM \\ k_t^{-2}h^{\alpha}(k_t) & \text{if } \alpha = TE \end{cases} \qquad \hat{\alpha}_{k,m}^{\alpha}(\underline{k}_t) = \begin{cases} \hat{\beta}_{k,m}^{\alpha}(\underline{k}_t) & \text{if } \alpha = TM \\ k_t^2\hat{\beta}_{k,m}^{\alpha}(\underline{k}_t) & \text{if } \alpha = TE \end{cases} \tag{22}$$

then equation 19 can be rewritten as

$$A_{k,m} = \sum_{j,\alpha} g^{\alpha}(k_{t;j})\hat{\alpha}^{\alpha}_{k,m}(\underline{k}_{t;j}) \tag{23}$$

The rate of convergence is governed by the behaviour of $g^{\alpha}(k_t)$ for large k_t. An asymptotic expansion for $g^{\alpha}(k_t)$ for large k_t can in general be written as

$$g^{\alpha}(k_t) \approx \tilde{g}^{\alpha}(k_t) = c_1^{\alpha}k_t^{-1} + c_2^{\alpha}k_t^{-3} + \ldots \tag{24}$$

From now onwards we will only consider a two-term asymptotic expansion for $g^{\alpha}(k_t)$ which will be more than sufficient for the acceleration. First, a so-called Kummer transformation step will be applied, where the asymptotically slow converging part of the general series will be substracted (resulting in fast converging reduced series) and added (resulting in slowly converging correction series).

$$A_{k,m} = \sum_{j,\alpha}[g^{\alpha}(k_{t;j}) - \tilde{g}^{\alpha}(k_{t;j})]\hat{\alpha}^{\alpha}_{k,m}(\underline{k}_{t;j}) + \zeta_{k,m} \qquad \zeta_{k,m} = \sum_{j,\alpha}\tilde{g}^{\alpha}(k_{t;j})\hat{\alpha}^{\alpha}_{k,m}(\underline{k}_{t;j}) \tag{25}$$

The rate of convergence for the first series in 25 is now improved from order $O(k_t^{-1})$ to order $O(k_t^{-5})$. However the second series is still slowly converging. Its simpler form, however, allows prospects of progress. Second, a special transformation step will be applied, where the asymptotically slow converging correction series will be converted into an integration over some ρ of exponentially fast converging series of the type $\exp(-k^2\rho^2)$. Inspired by Ewald's transformation, we introduce the identity

$$\frac{1}{k_t^n} = \frac{2\lambda}{\Gamma(n/2)}\int_0^{\infty}\rho^{\lambda n-1}e^{-k_t^2\rho^{2\lambda}}d\rho \tag{26}$$

where λ is an arbitrary positive parameter. The second series of equation 25 can now be written as

$$\zeta_{k,m} = \frac{2\lambda}{\sqrt{\pi}}\int_0^{\infty}\rho^{\lambda-1}\sum_{j,\alpha}(c_1^{\alpha} + 2\rho^{2\lambda}c_2^{\alpha})e^{-k_{t;j}^2\rho^{2\lambda}}\hat{\alpha}^{\alpha}_{k,m}(\underline{k}_{t;j})d\rho \tag{27}$$

This expression has the advantage that the series converges exponentially fast in k_t for $\rho > 0$ enabling a truncation to a finite interval $(0, \rho_2]$ for the infinite ρ-integration. Except near $\rho = 0$ the series still needs a relatively large number of terms for convergence. The evaluation of the integrand will therefore consist of two parts with a carefully chosen transition point ρ_1: one for an interval $[\rho_1, \rho_2]$ corresponding to large ρ which can be evaluated numerically very efficient

$$\int_{\rho_1}^{\rho_2}\rho^{\lambda-1}\sum_{j,\alpha}(c_1^{\alpha} + 2\rho^{2\lambda}c_2^{\alpha})e^{-k_{t;j}^2\rho^{2\lambda}}\hat{\alpha}^{\alpha}_{k,m}(\underline{k}_{t;j})d\rho \tag{28}$$

and one for an interval $(0, \rho_1]$ corresponding to small ρ for which we used a sophisticated evaluation method.

VALIDATION

The model has been validated by comparing the results (reflection behaviour of an arbitrary feed-radiator-frequency selective surface structure) with those generated by a commercial simulation package HFSS. A very close agreement has been obtained. These results have been published in a previous paper [4]. However the emphasis in this paper is on the acceleration technique for which we have considered some special applications consisting of rectangular geometries such as the strip, square, and gridded square chosen on an orthogonal grid. The expansion and weighting functions are simple rooftop functions, with an orientation in either the x or y direction.

For the original non-accelerated series 23 at least 3200 terms were needed to obtain an acceptable relative convergence of 10^{-2} for the admittance matrix. For the reduced series 25 only 10 terms were needed to obtain the same acceptable convergence. The integration over ρ has been evaluated numerically by using a Simpson's integration rule with only 43 points uniformly distributed over only a short interval from $\rho = 0$ to $\rho = \rho_2 = 0.7$ with transition point $\rho_1 = 0.17$. For the large ρ series 28 only 10 terms were needed to obtain the same acceptable convergence. The accurate result of the accelerated method is of equal order when compared to the non-accelerated method. However it is evaluated with a significantly lower amount of steps (factor 10).

CONCLUSIONS

First in this paper we have considered the analysis of stratified periodic electromagnetic field problems. These type of problems involve structures that can contain both waveguide as well as periodic layered space components. A ge neral theory is presented where these waveguide and periodic layered space components are treated equally. The model numerically solves a coupled system of two magnetic field integral equations by using the method of moment.

Second in this paper we have accelerated the calculation of the admittance matrix by making use of a combination of the Kummer and Ewald transformation. This acceleration technique has been implemented. In this case a significant acceleration (factor 10) is achieved while maintaining a high accuracy.

REFERENCES

[1] H. Blok, "Theory of Electromagnetic Waveguides," *Laboratory of Electromagnetic Research, Faculty of Electrical Engineering, Delft University of Technology*, 1995.

[2] A.T. de Hoop, "Radiation and Scattering of Electromagnetic Waves," *Laboratory of Electromagnetic Research, Faculty of Electrical Engineering, Delft University of Technology*, 1991.

[3] B.J. Morsink, S.W. Rienstra and A.G. Tijhuis, "Modeling Frequency Selective Surfaces with Multiple Metallization and Continuously Layered Dielectric Substrates," *24th ESTEC Antenna Workshop on Innovative Periodic Antennas : Photonic Bandgap, Fractal and Frequency Selective Structures,* ESTEC, 30/05/2001-01/06/2001, Noordwijk, The Netherlands.

[4] B.J. Morsink, G.H.C. van Werkhoven and A.G. Tijhuis, "A Coupled Feed-Radiator-Frequency Selective Surface Model for the Next Generation Active Phased Array Systems," *25th ESTEC Antenna Workshop on Satellite Antenna Technology,* ESTEC, 18/09/2002-20/09/2002, Noordwijk, The Netherlands.

[5] R. Orta, R. Tascone and R. Zich, "A Unified Formulation for the Analysis of General Frequency Selective Surfaces," *Electromagnetics*, vol. 5, no. 4, 1985, pp. 307-329.

[6] A.G. Tijhuis, "Plane-Wave Excitation of Two-Dimensionally Periodic Metallized Structures in Plane-Stratified Dielectric Media," *TUE Report of Study Contract for Thales Naval Netherland B.V.*, January 2002.